Acta Crystallographica Section B
Structural Science
ISSN 0108-7681

Comparison of the proton-transfer path in hydrogen bonds from theoretical potential-energy surfaces and the concept of conservation of bond order. II. $(N—H\cdots N)^+$ hydrogen bonds

Irena Majerz[a] and Ivar Olovsson[b]*

[a]Faculty of Chemistry, University of Wroclaw, Joliot-Curie 14, 50-383 Wroclaw, Poland, and [b]Department of Materials Chemistry, Ångström Laboratory, Box 538, SE-75121 Uppsala, Sweden

Correspondence e-mail: ivar.olovsson@mkem.uu.se

Received 12 March 2007
Accepted 5 May 2007

The quantum-mechanically derived reaction coordinates (QMRC) for the proton transfer in $(N—H—N)^+$ hydrogen bonds have been derived from *ab initio* calculations of potential-energy surfaces. A comparison is made between the QMRC and the corresponding bond-order reaction coordinates (BORC) derived by applying the Pauling bond-order concept together with the principle of conservation of bond order. We find virtually perfect agreement between the QMRC and the BORC for *intermolecular* $(N—H—N)^+$ hydrogen bonds. In contrast, for *intramolecular* $(N—H—N)^+$ hydrogen bonds, the donor and acceptor parts of the molecule impose strong constraints on the N—N distance and the QMRC does not follow the BORC relation in the whole range. The X-ray determined hydrogen positions are not located exactly at the theoretically calculated potential-energy minima, but instead at the point where the QMRC and the BORC coincide with each other. On the other hand, the optimized hydrogen positions, with other atoms in the cation fixed as in the crystal structure, are closer to these energy minima. Inclusion of the closest neighbours in the theoretical calculations has a rather small effect on the optimized hydrogen positions. [Part I: Olovsson (2006). *Z. Phys. Chem.* **220**, 797–810.]

1. Introduction

In a series of different crystalline compounds, where the same atoms X and Y are involved in the hydrogen bond $X—H—Y$, the distribution of the proton positions observed will be a result of perturbations of different magnitudes by the crystalline environment. However, the assembly of such points may be assumed to be distributed close to the minimum energy path for the transfer of a proton along this particular kind of hydrogen bond of the isolated system. This is the assumption behind the mapping of chemical reaction pathways from crystal structure data and which has been applied to a variety of crystal structures by Dunitz and collaborators (Dunitz, 1979; Bürgi & Dunitz, 1983). Based on this assumption, the ideal correlation curve for a particular type of hydrogen bond, $X—H\cdots Y$, can evidently be chosen as the minimum-energy proton-transfer path derived from the theoretical potential-energy surface of the system in question.

The concept of bond order has been popular in chemistry for a very long time and is often useful in 'explaining' systematic trends in the bond lengths in related compounds. In the previous paper (Olovsson, 2006) Pauling's bond-order concept was applied together with the principle of conservation of bond order to derive a simple functional representation of the interdependence of the $X—H$ and $H—Y$ distances in hydrogen bonds.

Table 1
Geometry of the hydrogen bonds (Å, °).

X-ray data: estimated uncertainty: N···N 0.01, N—H 0.05 Å, NHN 5°.

	N···N	N—H	H—N	N—H···N
BECHOG	2.608	1.30	1.30	180
ROHTIR	2.620	1.31	1.31	180
XOMFIO	2.878	1.44	1.44	180
QUKXEZ	2.664	1.33	1.33	180
LEQHIY	2.674	1.34	1.34	180
RULFAF	2.658	1.33	1.33	180
YULTOO	2.700	1.35	1.35	177
SAKKEU	2.587	1.30	1.30	173
HIDSAO	2.566	1.31	1.31	157
FEGQOX	2.614	1.46	1.46	128
KAHRIU	2.650	1.33	1.33	175
GERZUY	2.555	1.30	1.29	160
WERZAU	2.573	1.32	1.32	156
JACSAH	2.602	1.31	1.31	169

This function is called the BORC, bond-order reaction coordinate, in the following. Very good agreement between the BORC and the reaction coordinates derived from the quantum-mechanical calculations of potential-energy surfaces (QMRC) was found for HF_2^-, HCl_2^- and $H_3O_2^-$, as well as for H_3.

It is of great interest to investigate the agreement between the QMRC and the BORC for N—H—N hydrogen bonds also. No theoretical potential-energy surfaces appear to be available for this type of hydrogen bond (except for a simple model system; Toh *et al.*, 2001). In the present paper are presented the reaction coordinates QMRC from quantum mechanical calculations of potential-energy surfaces for a series of organic salts in which the cations form inter- or intramolecular $(N—H—N)^+$ hydrogen bonds. Here 14 organic compounds have been selected for the analysis. Although the compounds are chemically quite different all N—N distances, with one exception, are 2.6–2.7 Å (*cf.* Table 1). The data were taken from the Cambridge Structural Database (CSD; Allen, 2002); as the formulae are sometimes very complicated, the refcodes used in the database are also given in the figure texts. All structures were determined by X-ray diffraction (no neutron results are available for NHN hydrogen bonds). In six of these the NHN hydrogen bonds are *intermolecular*, in eight they are *intramolecular*.

2. Theoretical calculations

2.1. Potential-energy surfaces (PES)

Quantum chemical calculations were carried out at the B3LYP/6-31G(d,p) level of theory using the *Gaussian*03 (Gaussian Inc., 2004) system. The crystallographically determined coordinates for all atoms, except for the H atom involved in the hydrogen bond, were kept fixed and the potential-energy surface was generated for nitrogen–hydrogen distances successively changed in 0.04 Å steps. The proton was then moved along the $N_1—H$ and $N_2—H$ directions, where these directions were defined by the nitrogen and hydrogen positions taken from the structure determination. For computational reasons only the two molecules directly involved in the N—H—N hydrogen bonds are in most cases included in the calculation. This hydrogen-bonded complex is the cation with positive unit charge in each compound. The closest anion neighbours (with all their electrons) have also been included in the calculations for some of the simpler compounds to study the influence on the PES surface.

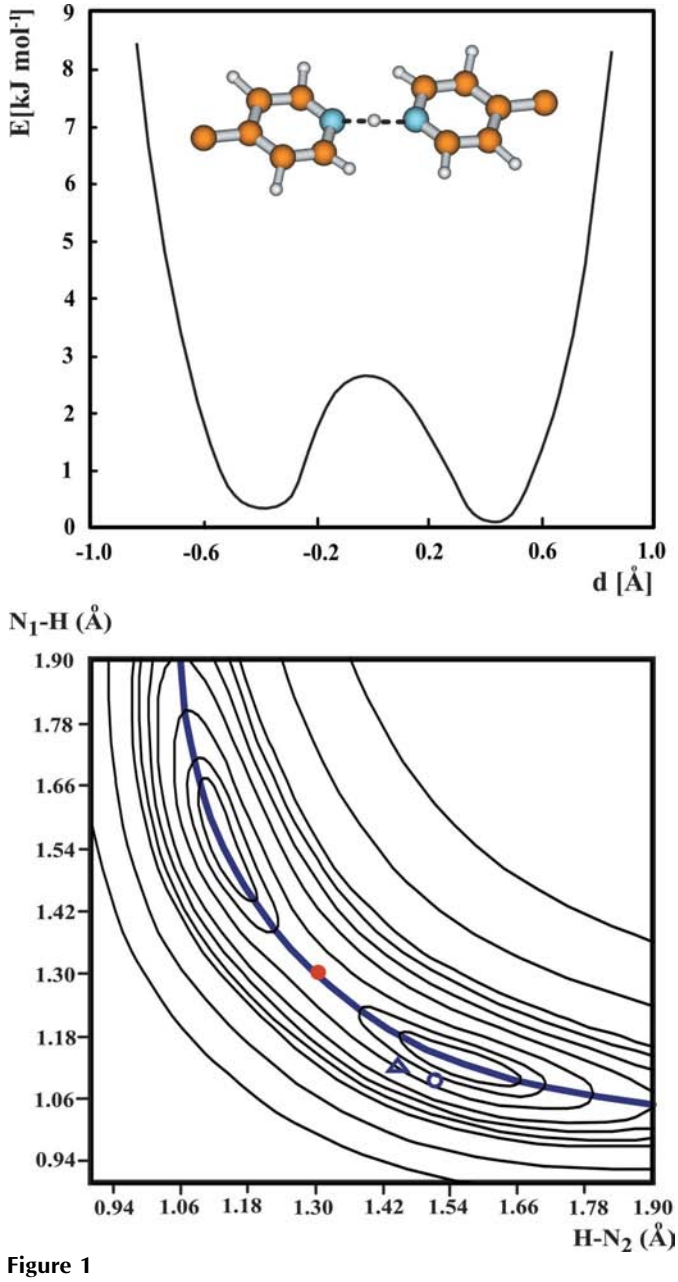

Figure 1
BECHOG: Geometry and potential-energy diagrams for the cation in the structure of bis(4-methylpyridine)hydrogen tetraphenylborate; space group *C*/*c* (Glidewell & Holden, 1982). The crystalline fragment used in the QM calculations is symmetric in this figure and all the subsequent figures. The upper part of the figure shows the complex considered explicitly in the QM calculations (methyl H atoms not shown) and the potential energy E as a function of $d = R(N_1H) - R(N_2H)$. The lower figure shows the two-dimensional QM-derived potential-energy map as a function of the $N_1—H$ and $N_2—H$ distances. Contour levels: 1, 2, 4, 8, 13, 17, 21, 42 and 84 kJ mol^{-1} (0.25, 0.50, 1, 2, 3, 4, 5, 10 and 20 kcal mol^{-1}).

The minimum-energy proton-transfer path has been derived by locating the points of lowest energy in the theoretical potential-energy diagram ('the reaction coordinates', QMRC) and fitting a curve through these points.

The X-ray determined position of the H atom is marked in the PES diagram as a *filled circle*; this position will be denoted H_{XD} in the following. As the structures have been determined by X-ray diffraction at room temperature, and are also rather complicated, these hydrogen positions are in many cases very uncertain. We estimate that the errors in the positions in some cases may amount to almost 0.05 Å.

2.2. Optimized hydrogen positions

The hydrogen position in the cation has also been optimized, with all other atoms in the cation fixed as in the crystal structure; the resulting hydrogen position is marked with a *triangle* in the PES diagram. For some of the complexes the closest anion neighbour has also been included (see above); this optimized hydrogen position is marked in the diagram with an *unfilled circle*. Furthermore, in GERZUY the *two* and in HIDSAU) the *eight* closest anions have also been included (with all their electrons); these optimized hydrogen positions

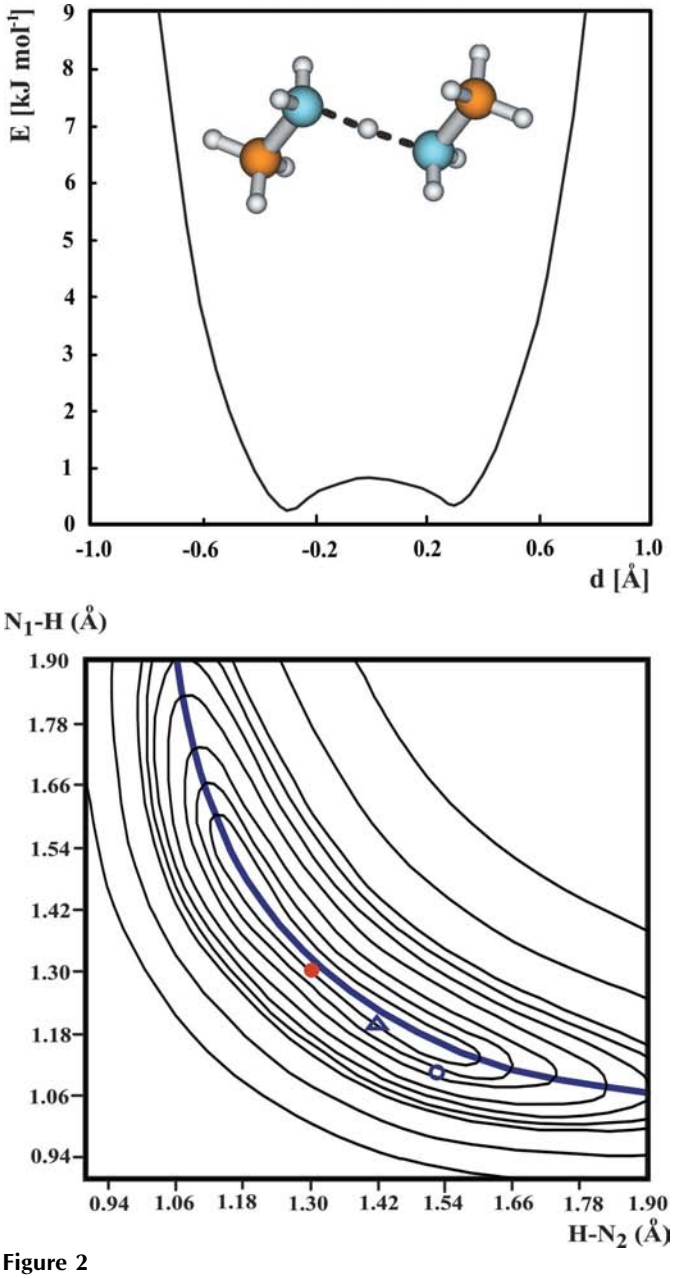

Figure 2
ROHTIR: The crystalline fragment (cation) taken from methylammonium methylamine tetraphenylborate at 200 K; space group $P\bar{1}$ (Bock *et al.*, 1997). Contour levels as in Fig. 1.

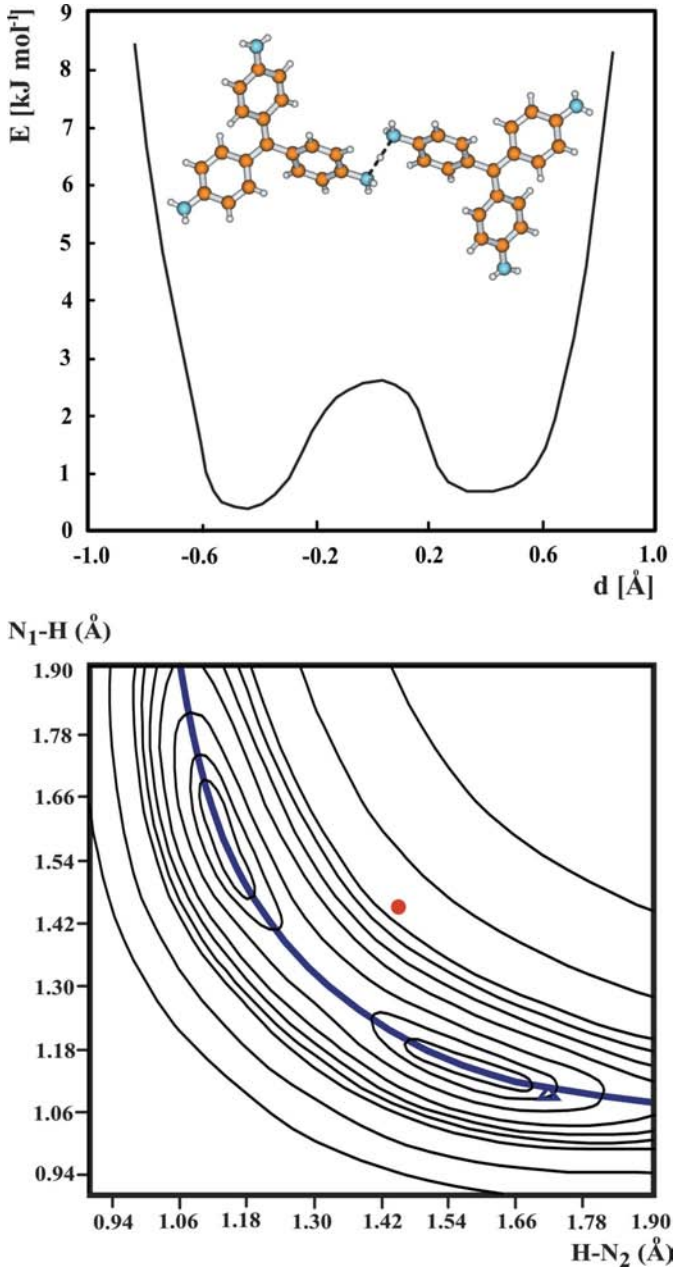

Figure 3
XOMFIO: [Hydrogen bis(tris(4-aminophenyl)carbenium)] (μ'-12-phosphato)tetracosakis(μ'-2-oxo)dodecaoxo-dodecamolybdenum at 173 K; space group $P\bar{1}$ (Liu *et al.*, 2002). Contour levels as in Fig. 1.

are marked with a *filled square* in the diagrams (*cf.* figure captions for details).

3. Bond order

Pauling (1947) introduced the idea that there is a simple relation between bond length and 'bond order' or 'bond valence'. This concept appears to be quite useful in many cases and attracts considerable interest even today (see *e.g.* Grabowski, 2000; Steiner, 2002; Mohri, 2005; Oláh *et al.*, 2006). Several expressions for this relation have been proposed (*cf.* Brown, 1992); the Pauling approach is as follows

$$d(\rho) - d(1) = \Delta d = -a \ln \rho, \quad (1)$$

where $d(\rho)$ is the interatomic distance for a fractional bond with bond order ρ and $d(1)$ is the corresponding single bond length. In a transfer reaction $X{-}H + Y \rightarrow X{-}H{-}Y \rightarrow X + H{-}Y$, it is postulated that the sum (n) of the bond orders ρ_1 and ρ_2 for $X{-}H$ and $H{-}Y$, respectively, will remain constant along the reaction coordinate. We thus obtain

$$\exp(-\Delta d_1/a_1) + \exp(-\Delta d_2/a_2) = n. \quad (2)$$

For the reactants, $d(\rho_1) = d(X{-}H, \text{free})$ and $d(\rho_2) = d(H\cdots Y, \infty)$, so that $\rho_1 = 1$ and $\rho_2 = 0$; for the products $\rho_1 = 0$, $\rho_2 = 1$. In a hydrogen bond the bond order of the two chemical bonds $X{-}H$ and $H{-}Y$ must add up to 1, so that $\rho_1 + \rho_2 = 1$ all along the reaction coordinate. The form of this curve is thus obtained from the Pauling relation under the condition that $\rho_1 + \rho_2 = 1$. We will refer to the curve thus calculated as the bond-order reaction coordinate (BORC).

Is it reasonable to assume that the sum of the bond orders remains constant along the reaction coordinate? In the previous paper (Olovsson, 2006) theoretical bond orders[1] from *ab initio* quantum-mechanical calculations were reported for the $[F{-}H{-}F]^-$ and $[HO{-}H{-}OH]^-$ systems using *Gaussian*03. From the theoretical calculations different bond orders may be derived and the definition of the bond order varies. For the $[F{-}H{-}F]^-$ system the Wiberg bond orders around the H atom vary from 0.645 to 0.660 (as F—H varies from 0.92 to 1.12 Å). For the $[HO{-}H{-}OH]^-$ system the bond orders are in the range 0.695–0.720. These results may be taken as justification for the above assumption that the sum of the bond order remains constant along the reaction coordinate, although the sum differs from one. Note also that this sum is not the same for the two systems tested (whereas it is assumed to be the same, and equal to one, in all cases in the Pauling approach). It may be remarked that the theoretically derived bond orders depend not only on their definition, but also on the partitioning of the electron density.

The selection of the parameters in the Pauling relation and derivation of the bond-order reaction coordinates (BORC) have been described in the previous paper (Olovsson, 2006). For NHN bonds the following reference distances were selected $d(\rho = 1) = 1.014$ Å (the spectroscopically determined equilibrium N—H distance in gaseous ammonia; Herzberg, 1950), $d(\rho = 0.5) = 1.30$ Å (half of the shortest N—N distance observed for linear and symmetric NHN bonds in crystals). These values give $a(\mathrm{N}) = 0.413$ Å. The BORC curve for NHN bonds is obtained by plotting $R(\mathrm{N_1H}) = 1.014–0.413\ln(1 - \rho)$ *versus* $\mathrm{R(N_2H)} = 1.014–0.413\ln\rho$, with ρ taken in suitable small steps.

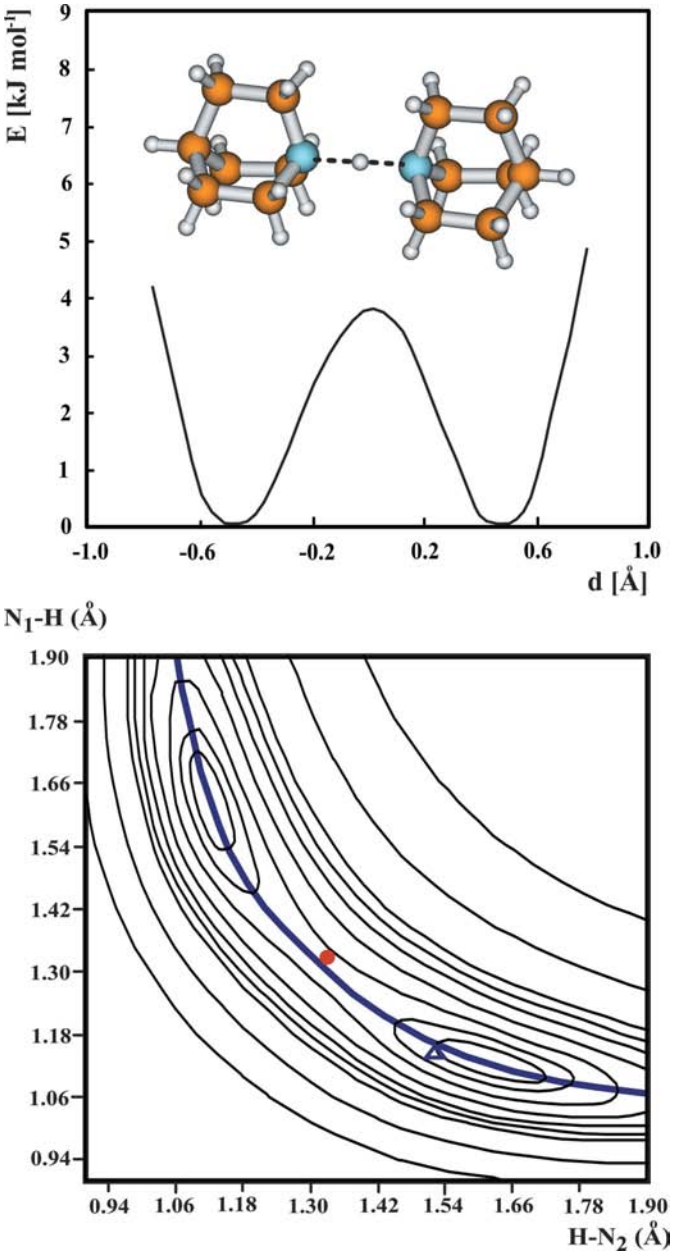

Figure 4
QUKXEZ: Hydrogen diquinuclidine chloride thiourea solvate at 298 K; space group *C*2/*c* (Yutronic *et al.*, 2001). Contour levels as in Fig. 1.

4. Results

In the lower part of Figs. 1–14 the potential-energy surface (PES) is presented as a function of the N_1H and N_2H distances

[1] In this work, theoretical bond order is the 'Wiberg bond order' in *Gaussian*03 (Wiberg, 1968; Mayer, 1986). This is calculated by the natural bond-orbital (NBO) analysis.

for the compounds studied here. The upper part of the figures shows the complex considered explicitly in the quantum-mechanical calculations and the potential energy E as a function of $d = R(N_1H) - R(N_2H)$. The contour lines of lowest energy in the PES are sometimes not shown in sufficient detail and the curves of E *versus* d then more clearly illustrate the characteristic features of the hydrogen-transfer process and in the case of double minimum potentials the relative energies of these minima [plotting against $d = R(N_1H) - R(N_2H)$ is chosen to give symmetric plots with respect to the H position in the middle of the bond when the environment is symmetric]. In a few cases E varies very strongly with d and a diagram with a larger energy scale has then been inserted.

4.1. Intermolecular N—H—N hydrogen bonds

The potential-energy diagrams are shown in Figs. 1–6, where the BORC curve is also drawn. The curve representing the minimum-energy proton-transfer path, QMRC, deviates < 0.01 Å from the BORC curve and is therefore not visible in the diagrams.

In all the diagrams there are double minima, but (except in Fig. 3) the X-ray-determined hydrogen positions, H_{XD}, are located at the saddle points according to the structure determinations. This is unexpected as in the case of double minima the H atom is often statistically distributed between the two minima around the symmetry centre, resulting in two half-hydrogen atoms in a diffraction study. However, in the present cases there is a large uncertainty in the hydrogen positions and furthermore the refinements of the X-ray data are not

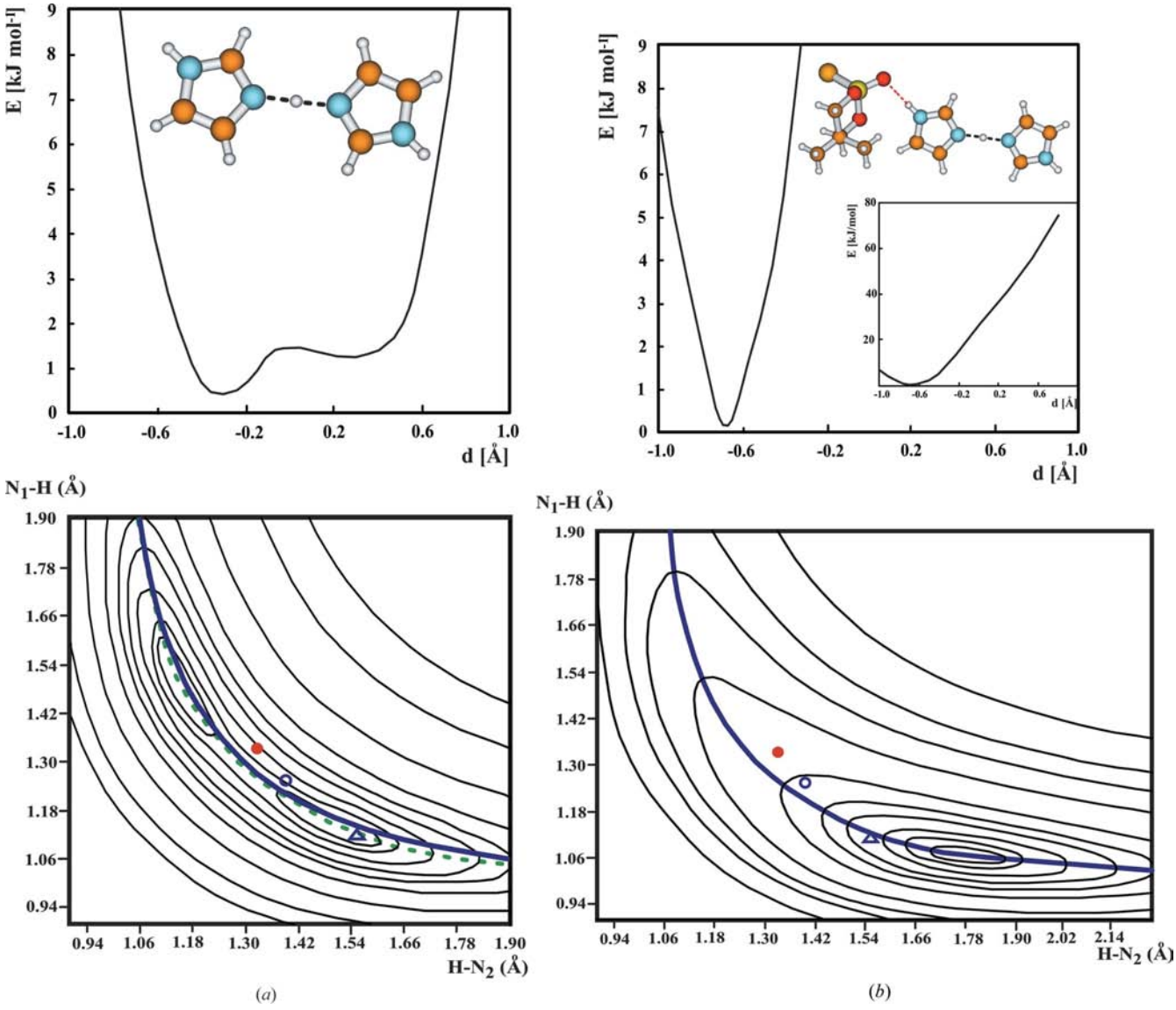

Figure 5
(*a*) LEQHIY: Bis(imidazole) 2-hydroxy-5,5-dimethyl-1,3,2-dioxaphosphorinane-2-sulfide; space group *I*2/*m* (Potrzebowski *et al.*, 1998). Contour levels: 1, 2, 4, 8, 13, 21, 42, 63, 84, 125 kJ mol^{-1} (0.25, 0.50, 1, 2, 3, 5, 10, 15, 20 and 30 kcal mol^{-1}). (*b*) LEQHIY with the closest anion (as shown) included in the calculations.

reported in sufficient detail to decide if the possibility of off-centred hydrogen positions has been tested. It is then interesting to notice that the optimized hydrogen position (triangle) is closer to one of the two energy minima (the optimization makes no distinction between the two minima). In Fig. 3 the H_{XD} atom is very far from the energy minimum; however, an extra H atom was also found in the experimental Fourier-difference map at the midpoint of the bond and with an occupancy of 0.5.

The strongest influence of the anion is seen for the intermolecular hydrogen bond in RULFAF and LEQHIY for which the anion changes the general shape of the potential-energy surface. In Figs. 5(*a*) and (*b*) (LEQHIY), the effect on the PES of including the closest neighbour (a complicated sulfide anion) in the calculations is demonstrated: the double minimum is changed to a single minimum and shifted. The corresponding results for RULFAF (Fig. 6) are very similar (not shown). The purpose of these figures is only to demonstrate the sensitivity of the PES and the proton position to the immediate environment. Naturally it is not possible from these results to draw any conclusions about the net effect if more distant neighbours are included in the calculations.

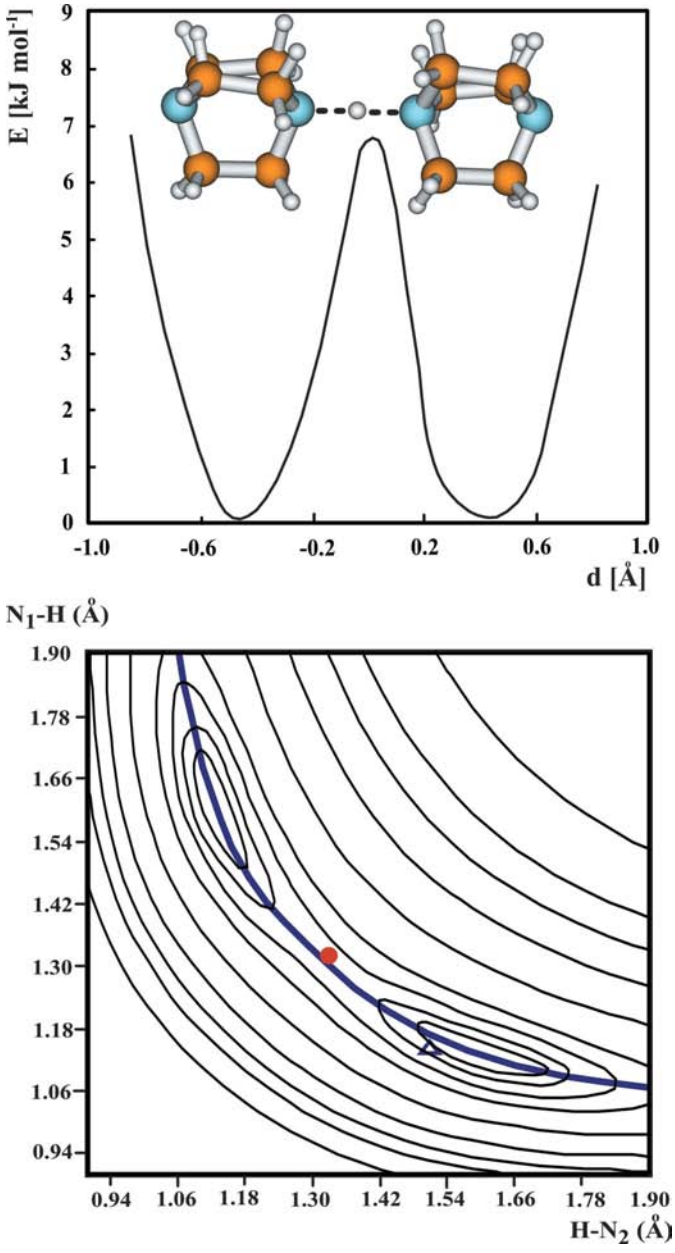

Figure 6
RULFAF: *catena*-([μ'-2-(1-aza-4-azoniabicyclo(2.2.2)octane](1,4-diazoniabicyclo(2.2.2)octane))-trichloro-nickel); space group *R*32 (Petrusenko *et al.*, 1997). Contour levels as in Fig. 5.

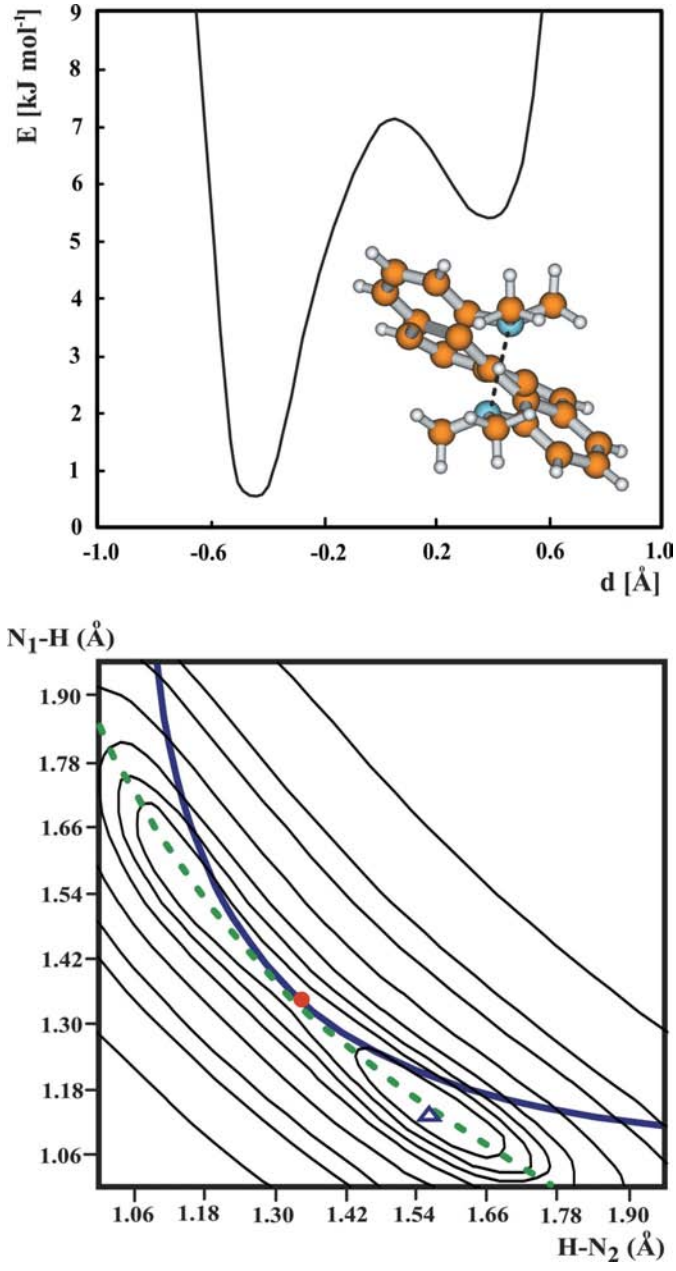

Figure 7
YULTOO: 1,12-Bis(dimethylamino)benzo(c)phenanthrene hydroiodide; space group *Pccn* (Staab *et al.*, 1995). Contour levels 4, 8, 13, 21, 42, 84, 125 and 293 kJ mol^{-1} (1, 2, 3, 5, 10, 20, 30 and 70 kcal mol^{-1}). The straight line fitted to the QMRC curve (dotted) has a slope of −1.08 (the equation of the line is $y = -1.08x + 2.83$, where $y = N_1H$ and $x = H{-}N_2$; $R^2 = 0.95$).

4.2. Intramolecular NH—N hydrogen bonds

The potential-energy diagrams for the selected intramolecular N—H—N hydrogen bonds are shown in Figs. 7–14. The minimum-energy proton path QMRC is marked as a dotted line and the BORC curve is drawn as a solid line. Here the BORC curve does not follow the QMRC and only in the central point does the BORC coincide with the QMRC. A probable reason for this discrepancy is discussed below in §5. As mentioned above, in all the intermolecular NHN hydrogen bonds there are symmetric double minima in the PES. In contrast, in the intramolecular NHN hydrogen bonds there is only one lowest minimum.

In all cases the QMRC is approximately a straight line; the slope of the fitted line is given in the figure text. A slope of −1.00 means that as N—H is decreased the distance of H—N is increased by the same amount to keep the N—N distance constant. A value more negative than −1.00 means that as N—

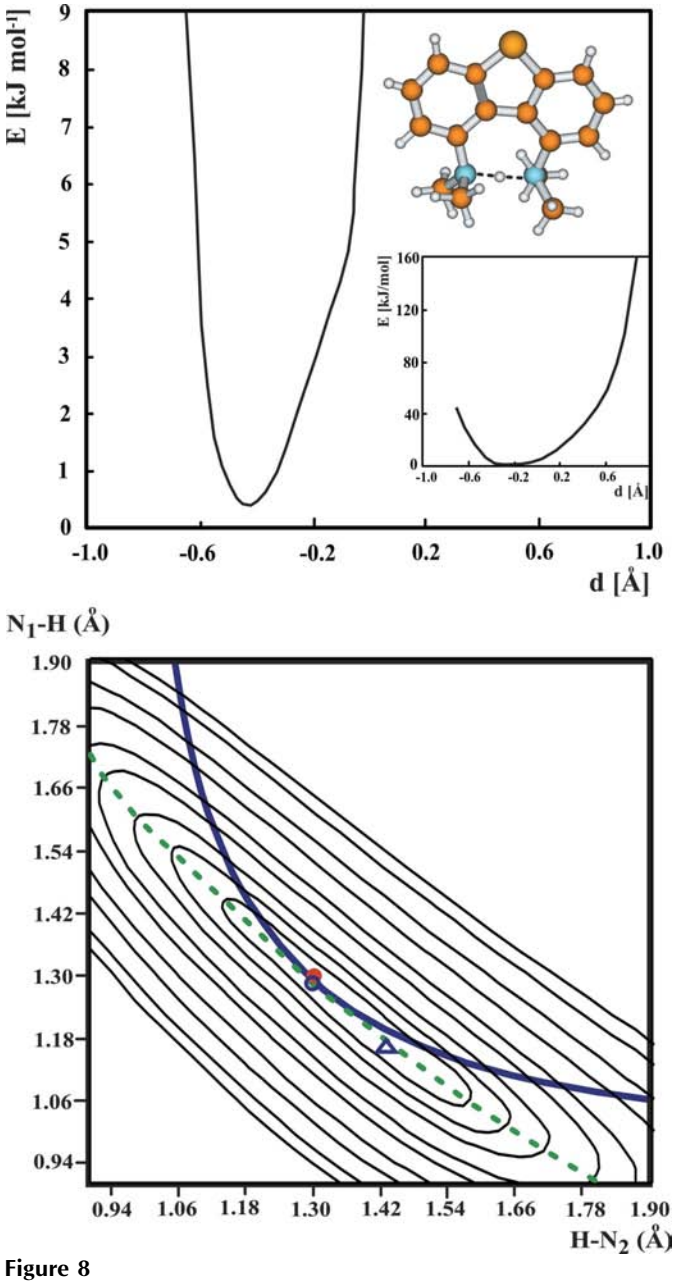

Figure 8
SAKKEU: 1-Dimethylamino-9-dimethylammoniodibenzothiophene tetrafluoroborate; space group *C*2/*c* (Staab, Hone & Krieger, 1988). Contour levels 8, 21, 42, 84, 125, 209, 293, 418, 502 kJ mol^{-1} (2, 5, 10, 20, 30, 50, 70, 100 and 120 kcal mol^{-1}). The straight line fitted to the QMRC curve has a slope of −0.90 (the equation of the line is $y = -0.90x + 2.83$, $R^2 = 0.95$).

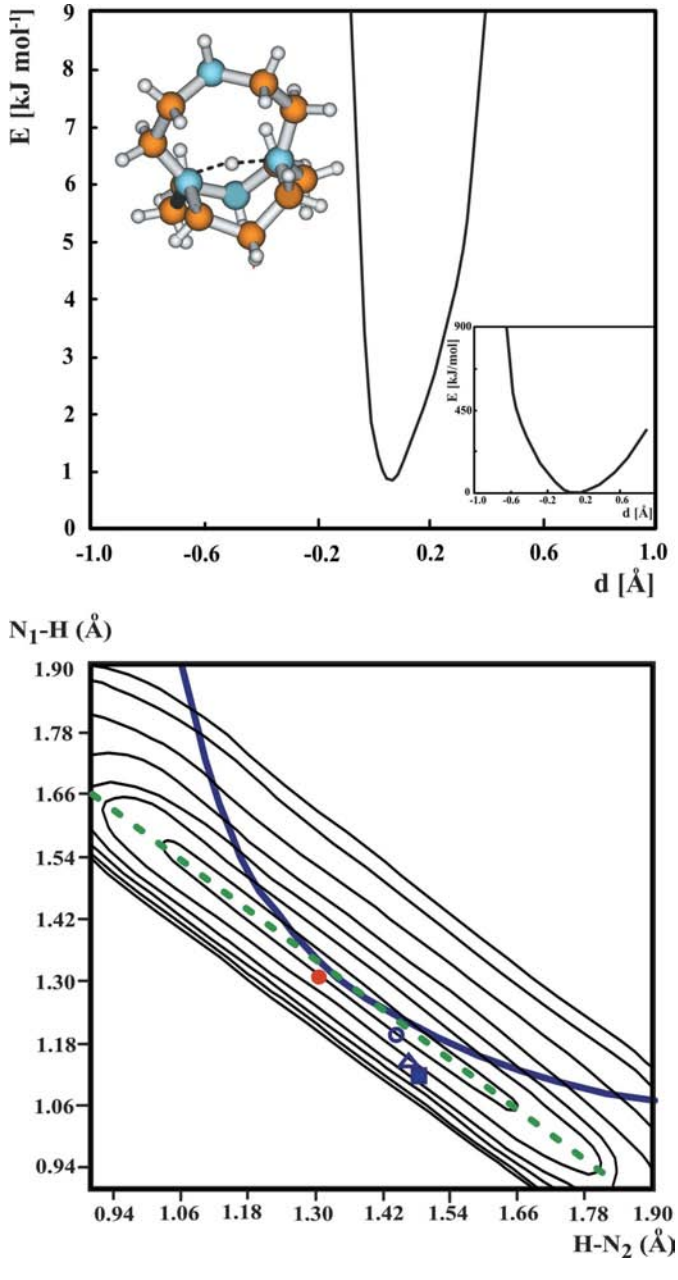

Figure 9
HIDSAO: 1,4,7,10-Tetra-azabicyclo(5.5.3)pentadecane dibromide perchlorate at 120 K; space group *Pnma* (Springborg *et al.*,1995). Contour levels 42, 84, 125, 209, 293, 418 and 502 kJ mol^{-1} (10, 20, 30, 50, 70, 100 and 120 kcal mol^{-1}). The straight line fitted to the QMRC curve has a slope of −0.79 (the equation of the line is $y = -0.79x + 2.34$, $R^2 = 1.00$). Note: in this case the unfilled circle corresponds to the optimized hydrogen position with one ClO_4^- and two Br^- ions as closest neighbours.

H is decreased the H—N distance only increases by a smaller amount. This implies that the originally bent NHN bond will become less bent. Correspondingly, when the slope is less negative than −1.00 the NHN bond will become more bent as the N—H distance is decreased (recall that the N—N distance is kept constant in all cases).

Whereas the energy levels in all the PESs for intermolecular hydrogen bonds are similar, those for intramolecular bonds differ significantly from one complex to another. The most drastic change in energy levels is seen in HIDSAO (Fig. 9). Here the PES is characterized by a very narrow, elongated minimum and for NH distances out of the minimum the energy strongly increases, especially with shortening of the NH distances. A similar shape of the PES is observed for JACSAH (Fig. 14). In both cases the hydrogen-bonded proton is located inside a cavity formed by three aliphatic chains which influences its mobility in the hydrogen bond.

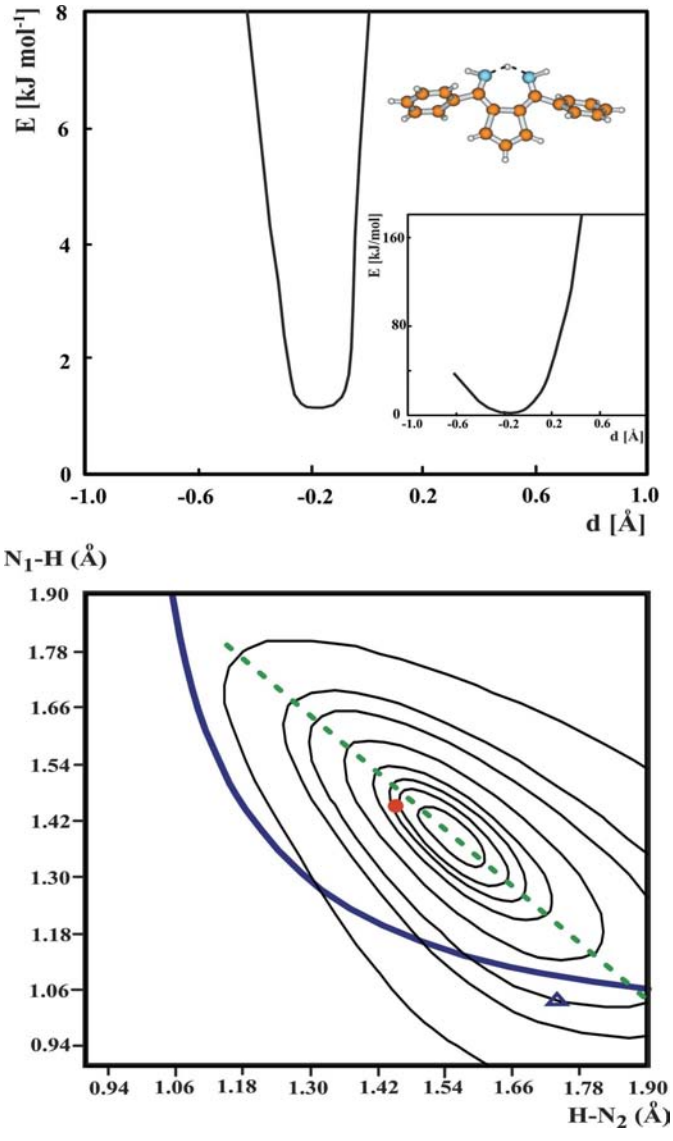

Figure 10
FEGQOX: 1,2-Cyclopentadienyldibenzylimine; space group $I4_1cd$ (Etkin *et al.*, 1998). Contour levels 4, 8, 13, 21, 42, 84, 125 and 293 kJ mol^{-1} (1, 2, 3, 5, 10, 20, 30 and 70 kcal mol^{-1}). The straight line fitted to the QMRC curve has a slope of −1.00 (the equation of the line is $y = -1.00x + 2.95$, $R^2 = 0.99$).

The next group of the PES with similar energy levels, lower than for HIDSAO and JACSAH but still higher than for intermolecular hydrogen bonds, is represented by SAKKEU, KAHRIU and WERZAU (Figs. 8, 11 and 13). Also in these cases the PES diagrams are characterized by one lowest minimum. All these cations have a similar structure which is a modification of a proton sponge.

For YULTOO, FEGQOX and GERZUY (Figs. 7, 10 and 12) the energy levels in the PES are close to those for the intermolecular complexes. The hydrogen bond in FEGQOX is far from linearity (NHN angle 128°) and this is reflected in the PES diagram with one distinct minimum, which can be reached for a limited range of NH distances. In such a bent hydrogen bond the proton cannot easily move from the central location. In this compound the QMRC and the BORC have no common central point as in the other complexes. This fact illustrates how far bent hydrogen bridges are from typical hydrogen bonds. The drastic difference between the QMRC and the BORC raises a question whether the interaction in FEGQOX should be considered as a hydrogen bond (although the N—N distance is only 2.61 Å). H_{XD} is very far from the N—N line and a strong interaction between the electron clouds of the proton and the donor/acceptor is then less likely. It may be pointed out that as a general principle the proton can be located at the N—H distances at which the QMRC coincides with the BORC. The central values of NH both curves in FEGQOX are very far from each other and a strong hydrogen bridge cannot be formed.

The influence of the anion (SCN^-) on the intramolecular hydrogen bond in WERZAU is significant (Figs. 13*a* and *b*), despite the shielding of the proton by the methyl groups around the N atoms. In the case of GERZUY (Figs. 12*a* and *b*), the proton is located in the centre of the cation and the presence of the anion ($CF_3SO_3^-$) only makes one part of the long minimum deeper. For KAHRIU (Figs. 11*a* and *b*) the Br^- ion does not influence the proton at all. Probably it is better shielded by the big molecule and the methyl groups and thus covers the space around the proton more effectively than in WERZAU.

It could be expected that the PES diagram for GERZUY (Fig. 12) would be similar to HIDSAO and JACSAH (Figs. 9 and 14) because of the similarity of the cation shape. However, the potential energy for this cation changes in a lower range and the minimum is less elongated. Small differences in the shape of the hydrogen-bonded cation will evidently influence the shielding and result in different possibilities of the proton moving.

The PES diagram of the intramolecular hydrogen bond in YULTOO (Fig. 7) is somewhat similar to the diagrams for intermolecular hydrogen bonds. There is a second minimum in the energy surface and the QMRC follows the BORC more closely than in the other intramolecular complexes. Evidently the proton has a larger freedom to move in YULTOO. The intermolecular hydrogen bond can be considered as a typical

hydrogen bond, in which the QMRC curve is identical to the BORC (the BORC is calculated without any constraints except that the sum of the bond orders remains constant along the reaction coordinate). The reason for the drastically different appearance of the potential-energy diagrams for intramolecular NHN bonds compared with the intermolecular ones is clearly that the donor and acceptor parts of the molecule impose strong constraints on the geometry of the hydrogen bond.

The fitted straight line of the QMRC in YULTOO has the lowest R^2 compared with the other intramolecular complexes. The R^2 value can be used as a measure of the similarity between the QMRC and BORC curves. If the QMRC is close to a straight line R^2 is close to one. When its shape becomes similar to the BORC the value of R^2 becomes lower. This is very well seen for the series of investigated complexes. R^2 changes from 1.00 for HIDSAO to 0.95 for YULTOO.

It is interesting to notice that the crystallographically determined hydrogen positions (H_{XD}, filled circles) are not located exactly at the theoretically calculated potential-energy minima but instead at the point where the QMRC and the BORC coincide. In contrast, the optimized hydrogen positions for the isolated cation (triangles), with other atoms in the cation fixed as in the crystal structure, are closer to the energy minima in the PES diagrams (except in FEGQOX, Fig. 10). Inclusion of the closest neighbours in HIDSAU (Fig. 9) as well

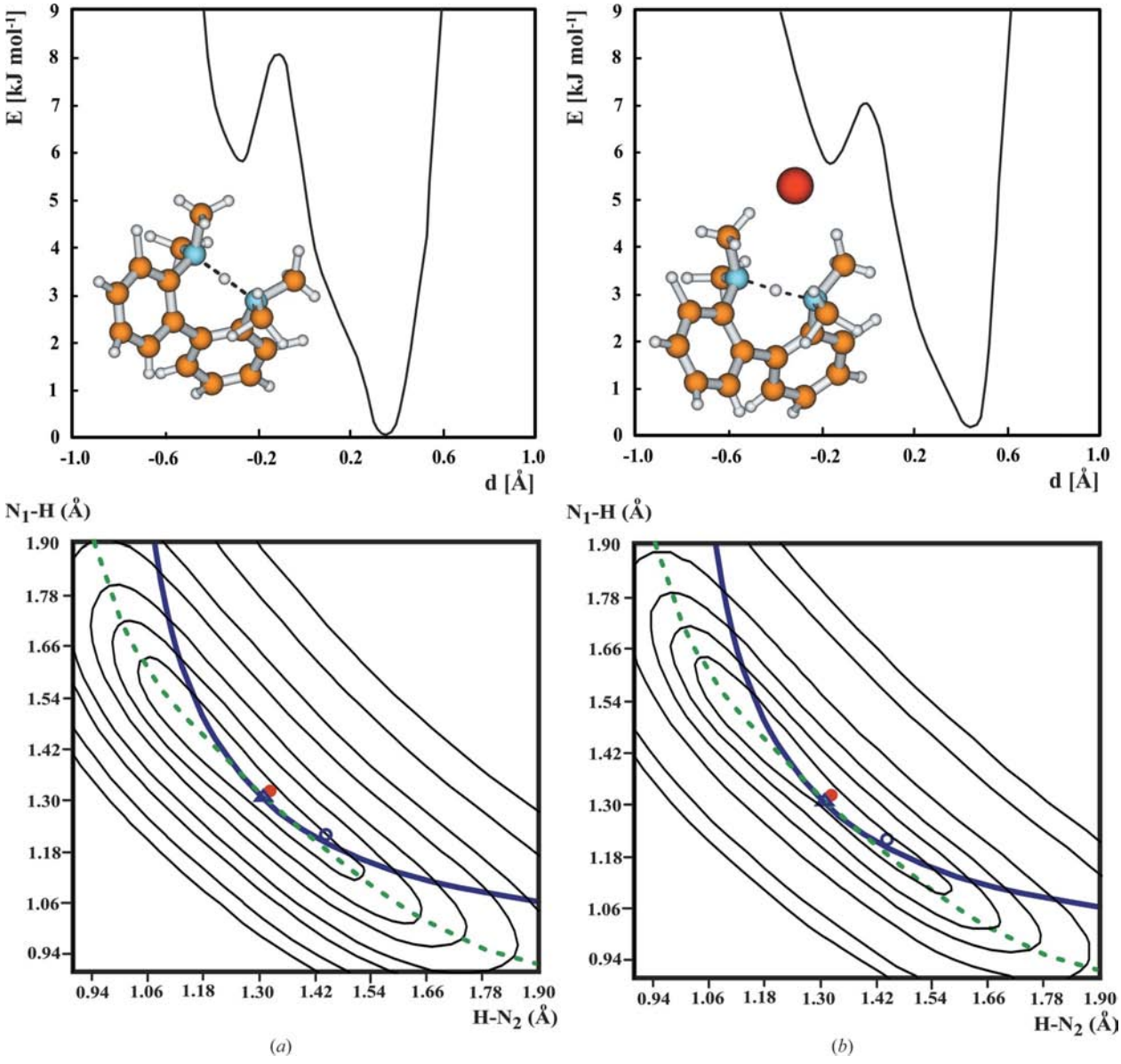

Figure 11
(a) KAHRIU: 2,2′-Bis(dimethylamino)biphenyl hydrobromide monohydrate. Space group $P2_12_12$ (Staab, Krieger & Hone, 1988). Contour levels 8, 21, 42, 84, 125, 209 and 293 kJ mol^{-1} (2, 5, 10, 20, 30, 50 and 70 kcal mol^{-1}). The straight line fitted to the QMRC curve has a slope of −1.05 (the equation of the line is $y = -1.05x + 2.74$, $R^2 = 0.98$). (*b*) KAHRIU with the closest neighbour (Br^-) included in the calculations.

as in GERZUY (Figs. 12*a* and *b*) has almost no influence on the optimized positions. For HIDSAU with one ClO_4^- and two Br^- ions as closest neighbours (open circles) as well with four ClO_4^- and four Br^- ions (filled squares), the positions are relatively close to each other. The same is true for GERZUY with one and two $CF_3SO_3^-$ anions (open circle and filled square, respectively). The reason for the relatively small effect of inclusion of the closest neighbours in the case of intramolecular hydrogen bonds is most likely that the hydrogen bond is more shielded in comparison to the situation in intermolecular hydrogen bonds.

5. Summary and general remarks

In all the intermoleclar NHN hydrogen bonds (Figs. 1–6) there are symmetric double minima in the PES (based on only the cation in the calculations). In contrast, in the intramolecular NHN hydrogen bonds (Figs. 7–14) there is only one lowest minimum; in a few cases there is a second minimum at a considerably higher energy (Figs. 7, 11, 12 and 14). Although some of the intramolecular bonds are also short (around 2.6 Å), the occurrence of double minima is evidently not dependent on the length of the hydrogen bond in these cases.

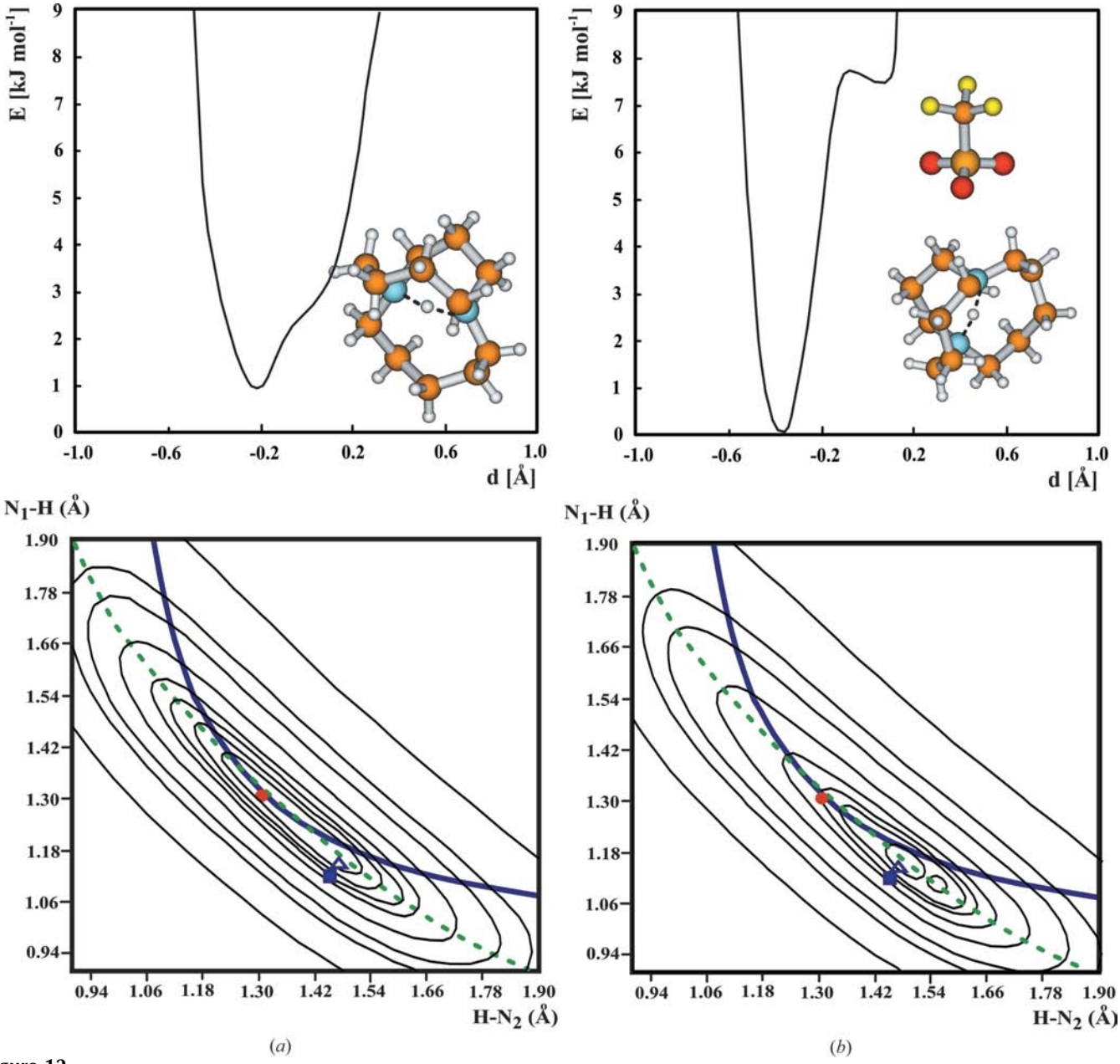

Figure 12
(*a*) GERZUY: 1,7-Diazabicyclo(5.4.3)tetradecane trifluoromethanesulfonate at 182 K; space group $P\bar{1}$ (White *et al.*, 1988). Contour levels as in Fig. 10. The straight line fitted to the QMRC curve has a slope of −0.98 (the equation of the line is $y = -0.98x + 2.63$, $R^2 = 0.99$). (*b*) GERZUY with its two closest neighbours ($CF_3SO_3^-$). The unfilled circle corresponds to the optimized hydrogen position with one $CF_3SO_3^-$ ion included in the calculations, the filled square with two $CF_3SO_3^-$ ions included.

For all the investigated compounds with intermolecular hydrogen bonds the QMRC coincides with the BORC, which is probably a general feature of intermolecular hydrogen bonds. In this case the proton can be located at all the NH lengths along the BORC. For intramolecular bonds (neglecting FEGQOX) only the central part of the QMRC coincides with the BORC so the proton can be located only around the hydrogen bridge center. For these complexes it is then interesting to note that the crystallographically determined hydrogen positions H_{XD} are not located exactly at the theoretically calculated potential-energy minima in the PES diagrams, but instead at the point where the QMRC and the BORC coincide. This appears to demonstrate the fundamental role that the principle of conservation of bond order plays in hydrogen bonds. The optimized hydrogen positions on the other hand are closer to the energy minima. However, in the above discussions the large uncertainty in the hydrogen positions determined by X-rays should be kept in mind.

In the five cases investigated the influence of the anions appears to be strongest for the intermolecular NHN bonds: the double minima in LEQHIY and RULFAF (Figs. 5 and 6) are for instance changed to single minima. This is to be expected as the hydrogen bond is in general more shielded in the intramolecular compounds. With the possible exception of

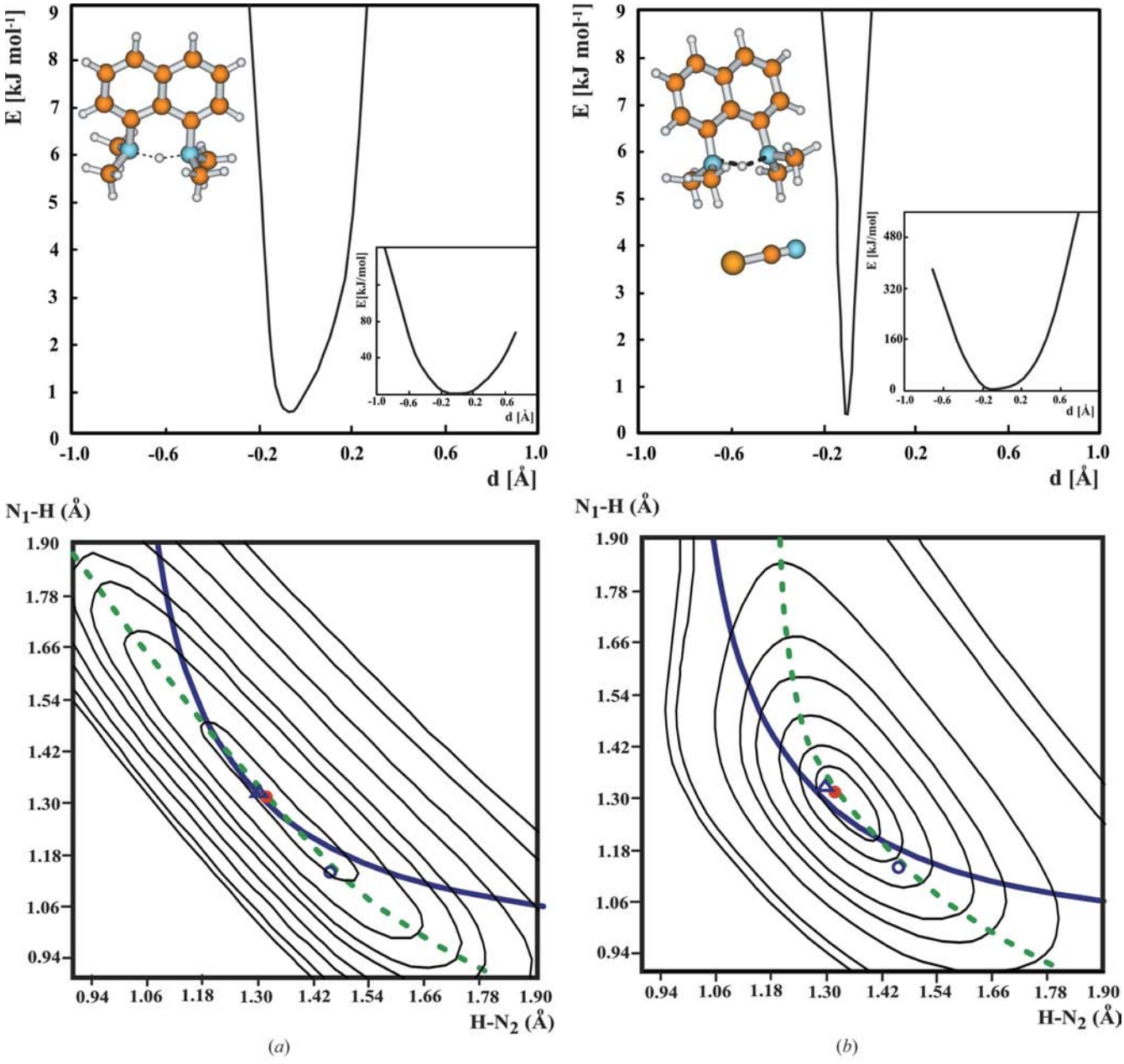

Figure 13
(*a*) WERZAU: 1,8-Bis(dimethylamino)naphthalene thiocyanate at 188 K; space group *Pbcn* (Bartoszak *et al.*, 1994). Contour levels as in Fig. 8. The straight line fitted to the QMRC curve has a slope of −1.17 (the equation of the line is $y = -1.17x + 2.91$, $R^2 = 0.99$). (*b*) WERZAU with the closest neighbour (SCN^-) included in the calculations.

XOMFIO (Fig. 3), the crystallographically determined hydrogen positions H_{XD} are rather close to the theoretically calculated potential-energy minima. However, it is very important to notice that in all the intramolecular complexes (except XOMFIO) H_{XD} is located at the point where the QMRC and the BORC coincide! The optimized hydrogen positions are close to the energy minima in the potential-energy surfaces. It appears that inclusion of the closest neighbour(s) in the theoretical calculations has a rather small effect on the optimized hydrogen positions.

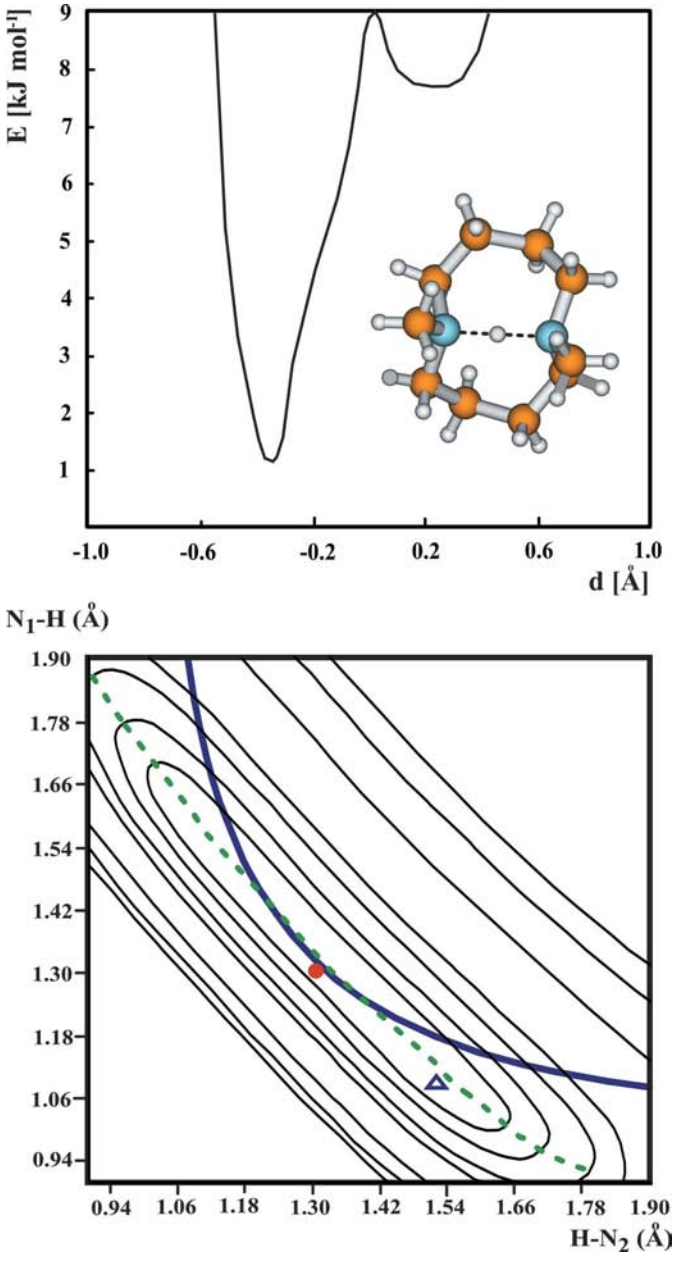

Figure 14
JACSAH: 1,6-Dimethyl-1,6-diazacyclododecane iodide dichloromethane solvate at 196 K; space group $R\bar{3}c$ (Alder *et al.*, 1988). Contour levels 21, 42, 84, 125, 293, 418 and 502 kJ mol^{-1} (5, 10, 20, 30, 70, 100 and 120 kcal mol^{-1}). The straight line fitted to the QMRC curve has a slope of −1.08 (the equation of the line is $y = -1.08x + 2.78$, $R^2 = 1.00$).

It appears that the potential-energy surface may be a useful tool to investigate how close the crystallographically determined hydrogen position is to the calculated energy minimum, which is determined only by the molecules directly involved in the bond. If all experimental and theoretical errors are excluded, the deviation of H_{XD} from the local energy minimum may be taken as a measure of the influence of the rest of the environment.

For compounds with intermolecular NHN bonds the bonding situation is evidently rather flexible so that the minimum-energy proton-transfer path, QMRC, follows very closely the BORC curve. The close agreement may seem rather surprising, considering the very simple assumption in the derivation of the BORC curve: the sum of the bond orders is equal to one all along the reaction path. It is notable that in two theoretically calculated bonds orders the sum is different from one and it also differs from one type of bond to another.

What is the reason for the agreement between the QMRC and BORC curves in the case of the intermolecular NHN bonds, and the disagreement in the intramolecular cases? Owing to the flexibility in the hydrogen-bond approach in the intermolecular compounds (Figs. 1–6) all these hydrogen bonds are linear. Also the Pauling bond-order approach and accordingly the derivation of the BORC curve are implicitly based on a linear hydrogen bond.

In the case of intramolecular hydrogen bonds the donor and acceptor parts of the molecule impose strong constraints on the N—N distance and accordingly on the geometry of the NHN bonds and as a consequence the hydrogen bonds cannot all be linear. The basic assumption in the derivation of the BORC curves is therefore not valid.

This work has been supported by a grant from the Trygger Foundation for Scientific Research. Professor Kersti Hermansson has contributed with very valuable suggestions. We thank the Wroclaw Centre for Networking and Supercomputing for generous computer time.

References

Alder, R. W., Eastment, P., Hext, N. M., Moss, R. E., Orpen, A. G. & White, J. M. (1988). *J. Chem. Soc. Chem. Commun.* pp. 1528–1530.
Allen, F. H. (2002). *Acta Cryst.* B**58**, 380–388.
Bartoszak, E., Jaskolski, M., Grech, E., Gustafsson, T. & Olovsson, I. (1994). *Acta Cryst.* B**50**, 358–363.
Bock, H., Vaupel, T. & Schodel, H. (1997). *J. Prakt. Chem.* **339**, 26–37.
Brown, I. D. (1992). *Acta Cryst.* B**48**, 553–572.
Bürgi, H. B. & Dunitz, J. D. (1983). *Acc. Chem. Res.* **16**, 153–161.
Dunitz, J. D. (1979). *X-ray Analysis and the Structure of Organic Molecules.* Ithaca, NY: Cornell University Press.
Etkin, N., Ong, C. M. & Stephan, D. W. (1998). *Organometallics*, **17**, 3656–3660.
Gaussian Inc. (2004). *Gaussian*03, Revision C.02, Gaussian, Inc., Wallingford, CT.
Glidewell, C. H. & Holden, D. (1982). *Acta Cryst.* B**38**, 667–669.

Grabowski, S. J. (2000). *J. Mol. Struct.* **552**, 153–157.
Herzberg, G. (1950). *Molecular Spectra and Molecular Structure.* New York: Van Nostrand.
Liu, G., Li, Q. & Zhang, S.-W. (2002). *Z. Anorg. Allg. Chem.* **628**, 1895–1898.
Mayer, I. (1986). *Int. J. Quantum Chem.* **29**, 73–84.
Mohri, F. (2005). *J. Mol. Struct.* **756**, 25–33.
Oláh, J., Blockhuis, F., Veszprémi, T. & Van Alsenoy, C. (2006). *Eur. J. Inorg. Chem.* pp. 69–77.
Olovsson, I. (2006). *Z. Phys. Chem.* **220**, 797–810.
Pauling, L. (1947). *J. Am. Chem. Soc.* **69**, 542–553.
Petrusenko, S. R., Sieler, J. & Kokozay, V. N. (1997). *Z. Naturforsch. B*, **52**, 331–336.
Potrzebowski, M. J., Cypryk, M., Michalska, M., Koziol, A. E., Kazmierski, S., Ciesielski, W. & Klinowski, J. (1998). *J. Phys. Chem. B*, **102**, 4488–4494.
Springborg, J., Kofod, P., Olsen, C. E., Toftlund, H. & Sotofte, I. (1995). *Acta Chem. Scand.* **49**, 547–554.
Staab, H. A., Diehm, M. & Krieger, C. (1995). *Tetrahedron Lett.* **36**, 2967–2970.
Staab, H. A., Hone, M. & Krieger, C. (1988). *Tetrahedron Lett.* **29**, 1905–1908.
Staab, H. A., Krieger, C. & Hone, M. (1988). *Tetrahedron Lett.* **29**, 5629–5632.
Steiner, T. (2002). *Angew. Chem. Int. Ed.* **41**, 48–76.
Toh, J. S.-S., Jordan, M. J. T., Husowitz, B. C. & Del Bene, J. E. (2001). *J. Phys. Chem. A*, **105**, 10906–10914.
White, J. M., Alder, R. W. & Orpen, A. G. (1988). *Acta Cryst.* C**44**, 662–664.
Wiberg, K. A. (1968). *Tetrahedron*, **24**, 1083–1096.
Yutronic, N., Jara, P., Manriquez, V., Wittke, O. & Gonzalez. G. (2001). CSD. Private communication.